Calculation of radiation loss in integrated-optic tapers and Y-junctions

R. Baets and P. E. Lagasse

Mode conversion and radiation loss in integrated-optic tapers and Y-junctions are calculated by means of the beam propagation method combined with the effective refractive-index method. Simple design rules for the tapers and Y-junctions are derived from the obtained results.

I. Introduction

In integrated optics Y-junctions can play a role as a multiplexer for wavelength division multiplexed systems or as an optical combiner for heterodyne detection systems. Devices based on an integrated Mach-Zehnder interferometer also contain Y-junctions. In all cases the problem usually is to design the junction so as to have a sufficiently low radiation loss while minimizing the use of area on the crystal. Each Y-junction contains a taper section. For this reason and because tapers are important devices in their own right, the first part of this paper deals with the problem of mode conversion and radiation losses in tapers, while Y-junctions are treated in the second part.

The light propagation through integrated-optic tapers and Y-junctions is calculated numerically using a combination of the beam propagation method (BPM) and the effective refractive-index method. The results of the purely numerical calculation are compared with results obtained from simple field overlap integrals. Special attention has been paid to the derivation of simple design rules for the tapers and Y-junctions.

II. Statement of the Problem and Calculation Methods

The waveguide geometry considered in this paper is sketched in Fig. 1. To restrict the number of possible geometries for the tapers and Y-junctions we assume that the refractive-index variation of the guide along the depth coordinate y is the same for the whole waveguiding structure and is chosen to allow only one guided mode in the depth direction. This is a reasonable approximation for most fabrication methods of strip guides. The refractive index $n(x,y,z)$ shows a large stepwise change at the air–substrate interface and slow and small variations within the substrate and the guide. This means that the modes are either quasi-TM or quasi-TE. The latter ones are to a very good approximation described by the scalar wave equation

$$\nabla^2 E_x + k^2 n^2(x,y) E_x = 0 \tag{1}$$

with appropriate boundary conditions.

The BPM can be used to solve Eq. (1) directly in 3-D.[1–3] However, for the waveguide geometries described above one can first reduce the problem to 2-D by means of the effective-index method. The BPM is then used to solve this 2-D problem. This simplification is justified by the fact that the z dependence of $n(x,y,z)$ for any x value is sufficiently small for the radiation in the depth direction to be negligible.

The effective-index method[4–6] consists of replacing $n(x,y,z)$ [Fig. 2(a)] for any value of x and z by $n_{\text{eff}}(x,z)$ which is the effective refractive index of the lowest-order mode of the slab guide with index variation $f(y) = n(x,y,z)$ [Fig. 2(b)]. The resulting structure [Fig. 2(c)] is y independent and can thus be solved in 2-D. The effective-index method has been used for several geometries of strip guides and has proved to provide accurate results in most cases. In the remaining part of this paper all waveguides will be directly described by their 2-D effective-index representation.

III. Radiation Loss and Mode Conversion in Symmetrical Tapers

The radiation loss of tapered waveguides has been investigated by several authors. Marcuse[7] has used a step approximation method for tapers in step waveguides. His approach was the basis for many other

The authors are with University of Gent, Laboratory for Electromagnetism & Acoustics, B-9000 Gent, Belgium.
Received 29 December 1981.
0003-6935/82/111972-07$01.00/0.

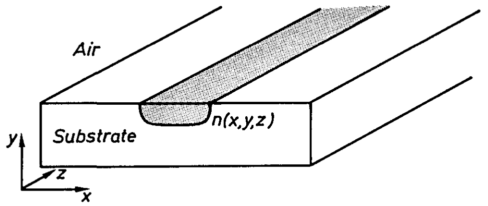

Fig. 1. Sketch of the geometry of the strip waveguides.

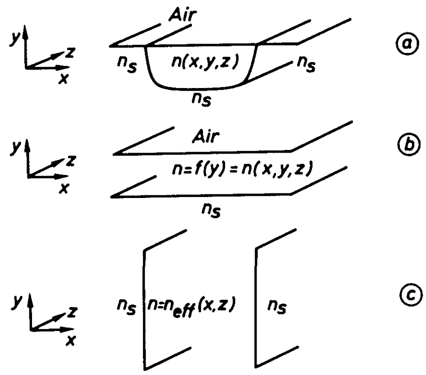

Fig. 2. Illustration of the effective-index method: (a) original 3-D profile; (b) slab waveguide used to calculate the effective refractive index for any value of x and z; and (c) resulting 2D effective profile.

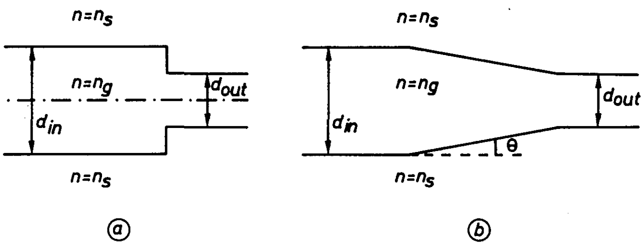

Fig. 3. Waveguide transition with n_g being the effective index of the guide: (a) abrupt transition, (b) tapering transition.

papers. Tzoar and Pascone[8] used an eikonal or local normal mode (LNM) approximation method. In this section the BPM is used to calculate the adiabatic power transfer between the fundamental modes of the input and output guides of a linear symmetric taper with step-index profile. If the transmission is perfectly adiabatic, the fundamental mode output power of the taper can be calculated as

$$p_{\text{out}} = \left| \int_{-\infty}^{\infty} \psi(x)\phi_{\text{in}}^{\star}(x)dx \right|^2, \tag{2}$$

where $\psi(x)$ is the field at the input of the taper, and $\phi_{\text{in}}(x)$ is the fundamental mode of the guide preceding the taper.

First, tapers with a reduction of 2 are considered here because of their importance in Y-junctions, but computations are also done for other ratios. Different horn shapes are described by several authors.[9-11] We will start with linear tapers but will be able to draw some conclusions for other geometries.

First, we consider the radiation loss of an abrupt transition between the waveguides [Fig. 3(a)]. Defining T_{00} as the power of the fundamental mode in the output guide when exciting the input guide with its normalized lowest-order mode, we can write to a good approximation

$$T_{00} = \left| \int_{-\infty}^{\infty} \phi_{\text{in}}(x)\phi_{\text{out}}^{\star}(x)dx \right|^2, \tag{3}$$

in which ϕ_{in} is the zeroth-order mode at the input, and ϕ_{out} is the zeroth-order mode at the output. It is assumed here that the changes in refractive index are smaller than a few percent so that reflections can be neglected.

Expression (3) was computed for different step-index profiles. These calculations show that T_{00} is dependent only on the normalized widths of the input and output guides, V_{in} and V_{out}, defined as

$$V_{\text{in}} = kd_{\text{in}}(n_g^2 - n_s^2)^{1/2},$$
$$V_{\text{out}} = kd_{\text{out}}(n_g^2 - n_s^2)^{1/2}. \tag{4}$$

Figure 4 shows T_{00} as a function of the geometric mean V_m of V_{in} and V_{out}, with $N = (V_{\text{in}}/V_{\text{out}})$, the reduction ratio, as a parameter. The regions where input and output guides are single mode are indicated. As Marcuse pointed out,[7] these curves show a minimum for particular V_m numbers. Moreover, this minimum appears at the same $(V_{\text{in}} \cdot V_{\text{out}})^{1/2}$ values for all reduction ratios. This value is ~2.5. For large values of N the minimum is very sharp, suggesting that these transitions could eventually be used to discriminate multiplexed signals with different wavelengths. Even for $N = 16$, the attenuation at the minimum is $\ngtr$0.25 dB. This should not be too surprising when looking at the effective normalized width of the fundamental mode of

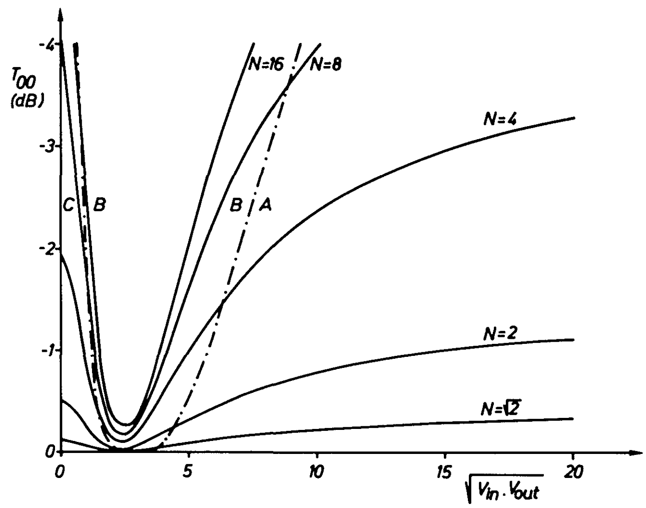

Fig. 4. Power transfer between fundamental modes in an abrupt transition for different reduction ratios: A, input guide multimode, output guide multimode; B, input guide multimode, output guide single mode; and C, input guide single mode, output guide single mode.

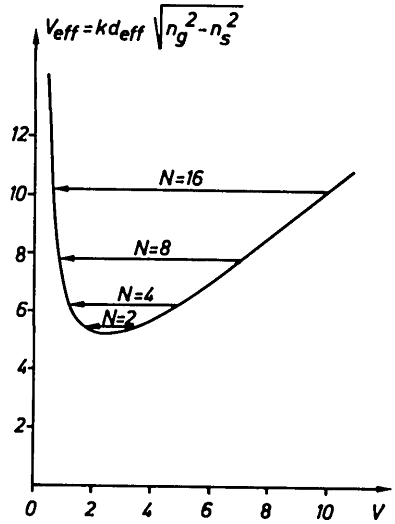

Fig. 5. Normalized effective width of a slab waveguide as a function of the effective width V.

a waveguide as a function of V, as shown in Fig. 5. The effective width d_{eff} has been defined here as the width between 12-dB points of the mode profile. This definition appeared to be most appropriate to compare the width of mode profiles of different shapes as involved here. As indicated in the figure, the minimum at $V_m = 2.5$ occurs when the effective normalized widths of the modes at input and output are equal.

Now we consider the case of a tapering transition. The refractive-index profile for the guides and the taper is assumed to be a step index. This has the advantage that exact analytical expressions for the modes exist, whereas for other profiles these have to be computed numerically.

Computation of T_{00} for tapers using the BPM shows that the radiation loss is dependent only on V_m [$= (V_{\text{in}} \cdot V_{\text{out}})^{1/2}$], $N = (V_{\text{in}}/V_{\text{out}})$, and $\sin\theta_{\text{eff}}$, with

$$\sin\theta_{\text{eff}} = \frac{\sin\theta}{\text{N.A.}}, \tag{5}$$

θ is the half-angle of the taper [Fig. 3(b)], and $\text{N.A.} = (n_g^2 - n_s^2)^{1/2}$, the numerical aperture. In Fig. 6(a), this dependence is drawn for $N = 2$ and in Fig. 6(b) for $N = 8$.

The figures show that the radiation loss for high $\sin\theta_{\text{eff}}$ values (short tapers) approaches that of the abrupt transition. For V_m values >2.5 the transmission loss can easily be reduced by choosing a sufficiently small taper angle θ. For $\sin\theta_{\text{eff}} < 0.1$, only a few percent of the input power is not transferred adiabatically. Figure 6(b) also shows that a taper can be worse than the abrupt transition if θ is not chosen small enough. This is particularly true in the region $V_m \simeq 2.5$ and for high N values. This can be explained by looking again at Fig. 5. In the case of the abrupt transition, V changed immediately from V_{in} to V_{out}, both of which correspond approximately to the same effective width. In the case of the taper, V changes slowly from V_{in} to V_{out}, which means that the effective width of the fundamental mode first decreases and then increases again. Unless θ is very small, this cannot be done without additional radiation loss.

Finally, in the region $V_m \ll 2.5$, where the guides are very weakly guiding, tapers have to be extremely slow. For the angles for which the calculations were done, the tapers are hardly better than the abrupt transition.

Although we have considered only linear tapers so far, we can draw some conclusions for other geometries from the previous results. For small values of N, one cannot

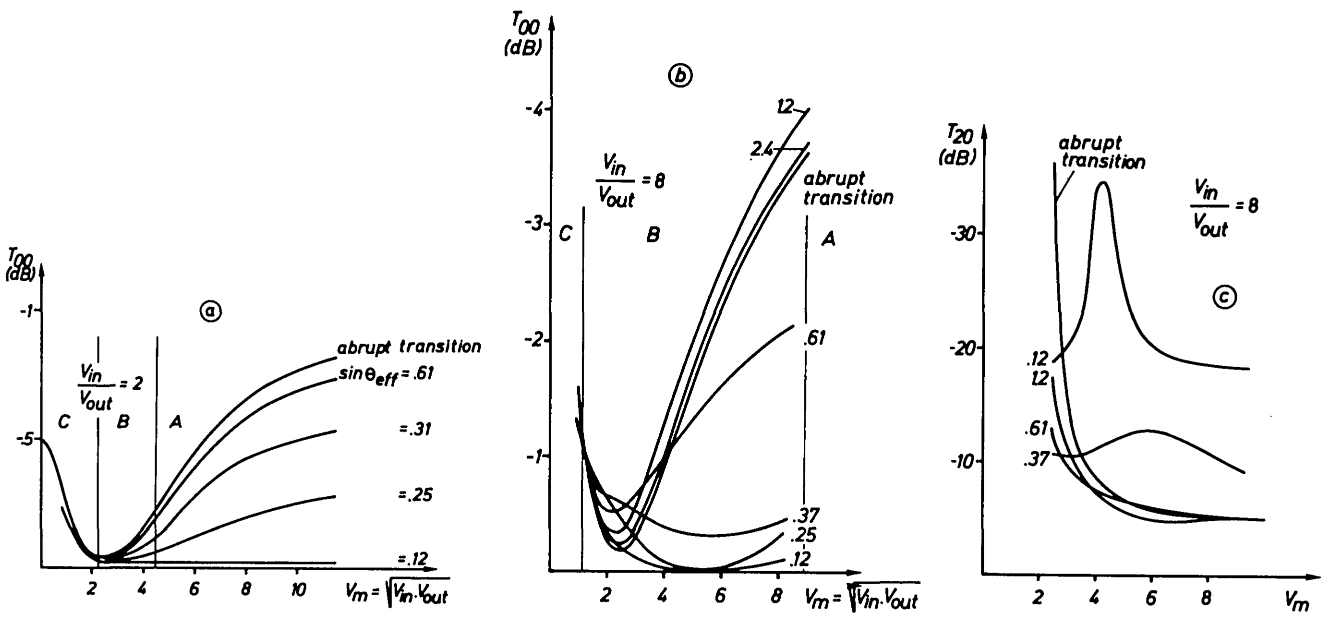

Fig. 6. Radiation loss and mode conversion in tapers for different values of parameter $\sin\theta_{\text{eff}}$. The regions A, B, and C are defined as in Fig. 4. (a) Power transfer between fundamental modes for a reduction ratio of 2. (b) As (a) for a reduction ratio of 8. (c) Conversion from second-order input mode to fundamental output mode for a reduction ratio of 8.

improve very much over linear tapers by choosing another shape. For large N values, however, we can find better taper design rules. In the region where $V_m > 2.5$, the results for $N = 2$ suggest that $\sin\theta_{\text{eff}}$ has to change approximately inversely proportional to V for the radiation loss to be constant. This means that, for a taper of large reduction ratio, the condition

$$\sin\theta_{\text{eff}} \cdot V(z) = \text{constant} \tag{6}$$

has to be fulfilled along the taper for the radiation loss to be equally divided over its total length. This implies that the shape of the taper will be quadratic. The constant in Eq. (6) should be <1.0 for the radiation loss to be smaller than a few percent. This design rule is only valid, of course, as long as $V_{\text{out}} > 2.5$. Condition (6) is in good agreement with the criteria proposed in Ref. 10.

A description of the properties of a taper should also include power conversion between modes. For a symmetrical linear taper with single-mode output the conversion from higher-order even modes at the input to the output mode has been calculated by means of the BPM for various taper angles. Figure 6(c) shows T_{20}, the output power in the fundamental mode for a normalized second-order mode at the input, for $N = 8$. As can be seen from comparison of Figs. 6(b) and (c), T_{20} is small when T_{00} is high and vice versa. This is in agreement with the requirement $T_{00} + T_{20} \leqslant 1$, which follows from reciprocity. Finally, Figs. 7(a)–(d) show the field amplitude in a linear taper for different modes as input fields. The figures show clearly how the lowest-order mode is converted to the input mode and how the higher-order modes radiate.

IV. General Properties of *Y*-Junctions

The relationship between the propagating fields in planes A and B of a Y-junction (Fig. 8) can be described by an S-matrix. Namely, each propagating mode in plane A resp. B can be considered as a port in a multiport structure. In the following discussion only propagating modes, both guided and radiating, are considered in planes A and B.

Figure 9 shows the Y-junction as a multiport. Since radiating ports are included in the derivation, the number of gates is in fact infinite.

With the notation of Fig. 9, we obtain

$$\begin{bmatrix} \bar{b}_A \\ \bar{b}_B \end{bmatrix} = \bar{\bar{S}} \cdot \begin{bmatrix} \bar{a}_A \\ \bar{a}_B \end{bmatrix}. \tag{7}$$

Assuming that the refractive-index changes are small enough so that reflections are negligible and taking reciprocity into account, the S-matrix takes the form

$$\bar{\bar{S}} = \begin{bmatrix} 0 & \bar{\bar{S}}_{AB}^{T} \\ \bar{\bar{S}}_{AB} & 0 \end{bmatrix}. \tag{8}$$

We also assume that the two waveguides in plane A have the same refractive-index profile and that these guides as well as the output guide have single-mode properties.

Defining $S_e = |S_e| \exp(j\theta_e)$ as the S-coefficient between the fundamental (even) input mode $\phi_e(x)$ and the guided output mode and $S_o = |S_o| \exp(j\theta_o)$ as the S-coefficient between the first-order (odd) input mode $\phi_o(x)$ and the guided output mode, passivity and reciprocity assure that $|S_e|^2 + |S_o|^2 \leqslant 1$. If the distance L between guides I and II is sufficiently large so that coupling can be neglected, $\phi_e(x)$ and $\phi_o(x)$ can be written as

$$\phi_e(x) = \frac{1}{\sqrt{2}} \psi\left(\frac{L}{2} + x\right) + \frac{1}{\sqrt{2}} \psi\left(\frac{L}{2} - x\right), \tag{9}$$

$$\phi_o(x) = \frac{1}{\sqrt{2}} \psi\left(\frac{L}{2} + x\right) - \frac{1}{\sqrt{2}} \psi\left(\frac{L}{2} - x\right), \tag{10}$$

in which $\psi(x)$ is the fundamental mode of one separate input guide. Excitation of guide I by its fundamental mode provides a guided output with amplitude $(1/\sqrt{2})\,|S_e + S_o|$, whereas excitation of guide II provides an output $(1/\sqrt{2})\,|S_e - S_o|$.

By multiplying the two corresponding output powers, we get

$$\begin{aligned} &(\tfrac{1}{2}|S_e + S_o|^2) \cdot (\tfrac{1}{2}|S_e - S_o|^2) \\ &\quad = \tfrac{1}{4}[(|S_e|^2 + |S_o|^2)^2 - 4|S_e|^2|S_o|^2 \cos^2(\theta_e - \theta_o)] \\ &\quad \leqslant \tfrac{1}{4}[1 - 4|S_e|^2|S_o|^2 \cos^2(\theta_e - \theta_o)] \leqslant 1/4. \end{aligned} \tag{11}$$

As to a symmetric Y-junction for which $S_o = 0$, we conclude that there is always a minimum 3-dB loss. This minimum is obtained when the even mode $\phi_e(x)$ in plane A is converted adiabatically to the output guided mode. For an asymmetric Y-junction, Eq. (11) shows that the average of the attenuation (in decibels) over the two input guides is always worse than 3 dB, i.e.,

$$\tfrac{1}{2}(10 \log \tfrac{1}{2}|S_e + S_o|^2 + 10 \log \tfrac{1}{2}|S_e - S_o|^2) \leqslant -3 \text{ dB}. \tag{12}$$

More generally, for a structure connecting M single-mode and uncoupled guides to one single-mode output guide, this average (in decibels) per input guide is always minimum $10 \log M$ dB.

As indicated in Fig. 8 the Y-junction can be subdivided into two regions: a region in which the input guides approach each other and start coupling and, second, a taper. The results obtained in a previous paragraph allow us to design the taper section of the Y-junction in such a way as to minimize the radiation losses. This means that in the next section we will concentrate on the problem of the coupling region of the Y-junction.

V. Radiation Loss in *Y*-Junctions

The first part of the Y-junction should be designed so that it transfers the power of the even mode $\phi_e(x)$ adiabatically to the even fundamental mode at the entrance of the taper. Computations were done for three different configurations. The first one has straight input guides as shown in Fig. 10(a). For this Y-junction and also for the other ones described in this section, the input and output guides have an effective-index profile as drawn in Fig. 11. These guides are single mode at $\lambda = 1.3\ \mu$m. The whole Y-junction is designed so that all index variations are slow. The junction of Fig. 10(a) has oblique input guides. To start from parallel input

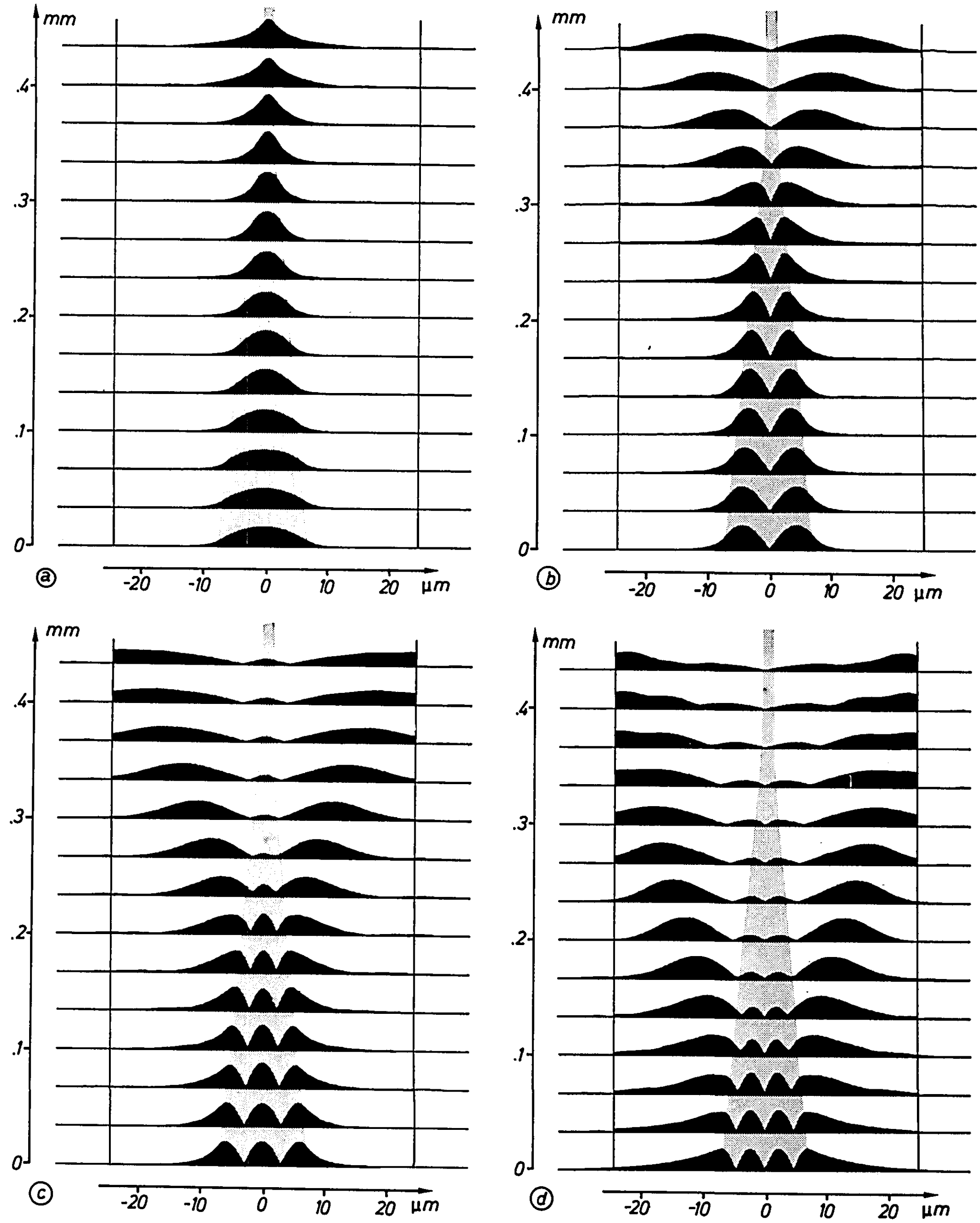

Fig. 7. Field amplitude in a taper with $V_{in} = 10$ and $V_{out} = 1.25$, $\theta = 1°$, $n_g^2 - n_s^2 = 0.02$, $n_s = 1$, $\lambda = 1.3\ \mu m$. (a) Lowest-order mode at the input. (b) First-order mode at the input. (c) Second-order mode at the input. (d) Third-order mode at the input.

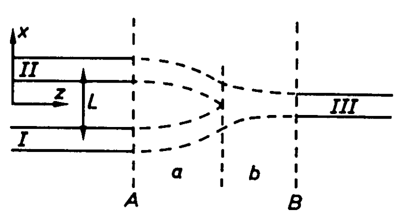

Fig. 8. Y-junction configuration.

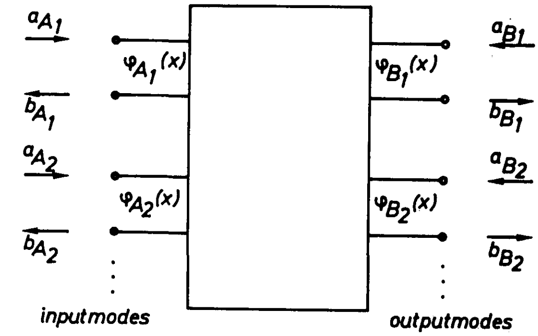

Fig. 9. Representation of the Y-junction as a multiport.

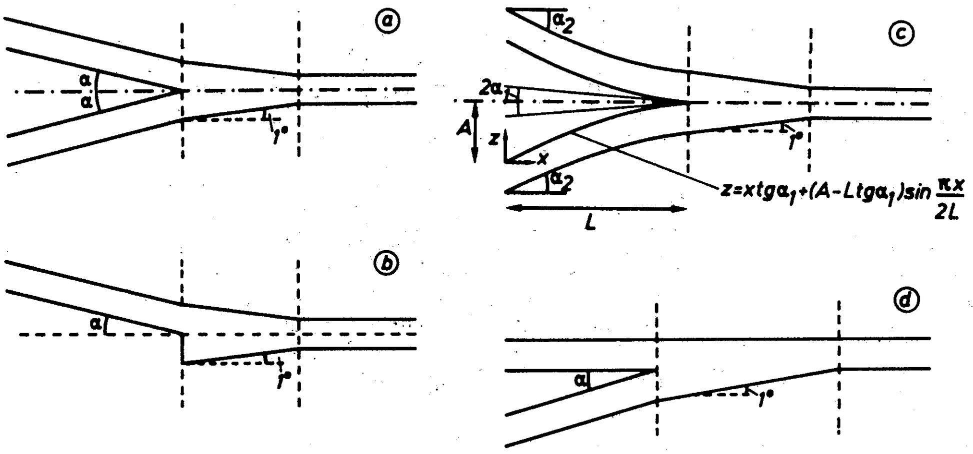

Fig. 10. Y-junction configurations: (a) straight input guides; (b) as (a), one input guide missing; (c) bent input guides; (d) nonsymmetrical junction.

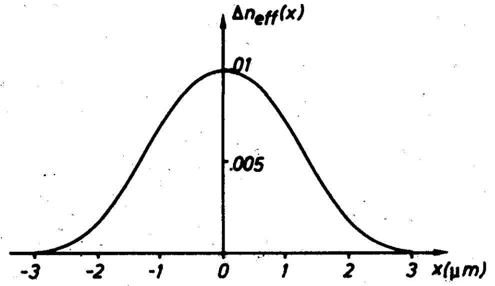

Fig. 11. Effective refractive index $n_g - n_s$ ($n_s = 1$).

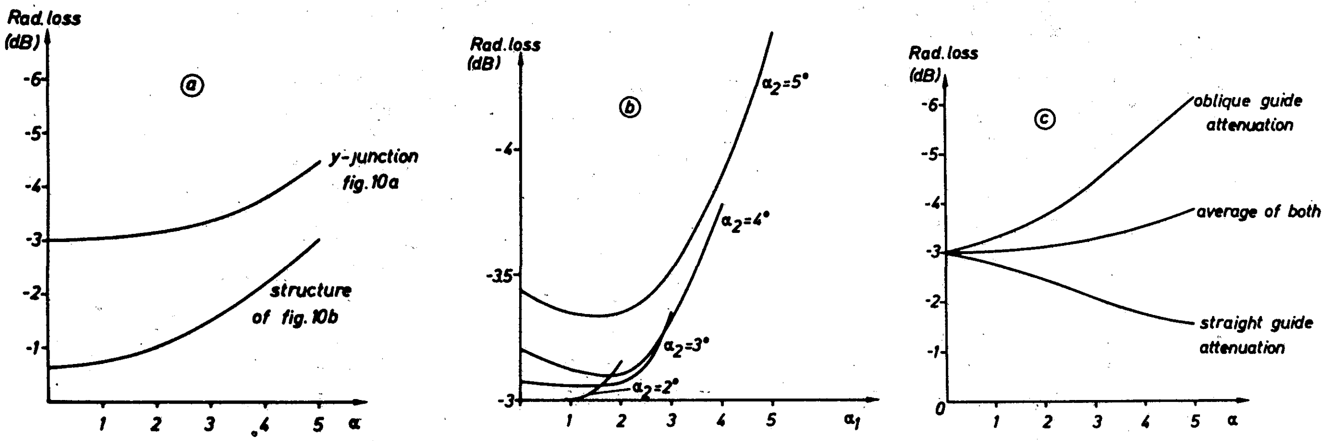

Fig. 12. Radiation loss in Y-junctions: (a) straight guides; (b) bent guides; (c) nonsymmetrical guides.

guides as in Fig. 8, bends have to be added which give an additional radiation loss. These bends are described in Ref. 12.

Figure 12(a) shows the radiation loss of a complete Y-junction as in Fig. 10(a). The taper was designed to be adiabatic. One input guide is excited with its fundamental mode, and the power at the input of the Y-junction is computed using the BPM. It is interesting to compare these results with the configuration of Fig. 10(b), which is identical with the one of Fig. 10(a) except for the missing second input guide. As can be seen from Fig. 12(a), these radiation loss values are <3 dB. This emphasizes the influence of the symmetry in the structure.

Figure 12(a) also shows that the loss beyond 3 dB for the Y-junction increases approximately quadratically with the angle α. This implies that this angle has to be small and thus that the region where the input guides couple has to be long. Therefore a Y-junction with curved input guides, as shown in Fig. 10(c), was investigated. The distance A was 8λ, enough for the coupling between the guides at the input to be very low. The results are shown in Fig. 12(b). The radiation loss is plotted as a function of α_1 with α_2 as a parameter. The minimum in these curves is a trade off between minimal angle α_1 and minimum bend losses. If 3.10 dB is considered as a reasonable value for the radiation loss, $\alpha_1 = 2°$ and $\alpha_2 = 4°$ are good choices. The coupling

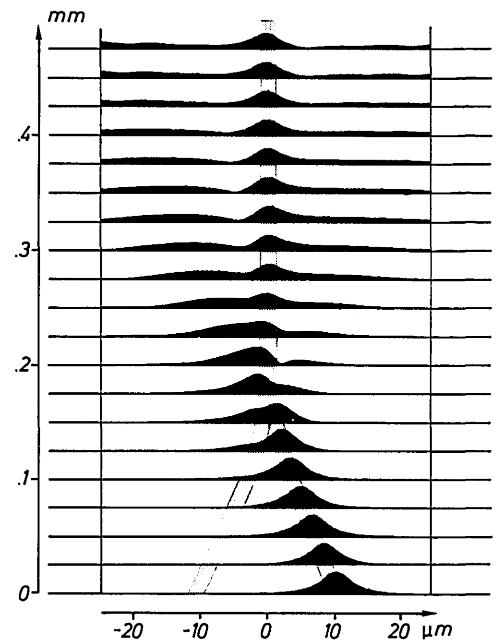

Fig. 13. Field amplitude in a Y-junction as in Fig. 10(c): $\alpha_1 = 2°$, $\alpha_2 = 4°$, $\lambda = 1.3\ \mu$m.

region between the input guides for this configuration is two to three times shorter than the equivalent case with straight guides. Figure 13 shows the field amplitude in a Y-junction of this type.

In most practical cases the two input guides will be parallel and must be brought together by bends. If the original spacing between them is large ($\gg 10\lambda$), a long distance will be needed to bring them together with reasonable loss. The space taken by the bends will exceed the space taken by the Y-junction. Finally, radiation loss in a nonsymmetric junction [Fig. 10(d)] was calculated. Figure 12(c) shows the radiation loss from both sides and their average. As predicted by theory, this average always exceeds 3 dB.

VI. Conclusion

The guided power at the output of a taper with single-mode output guide can easily be calculated by computing a modal expansion of the field at the input and by taking the lowest-order component, if this taper behaves adiabatically. The taper angle required for such adiabatic behavior depends strongly on the V numbers of input and output guides as shown in Fig. 6. For $V_{out} > 2.5$ the angle has to be chosen inversely proportional to V_m. For a V_m value of $\sim$2.5, the angle may be large, and even abrupt transitions can eventually give satisfactory results. The BPM has proved to be a very convenient technique for computation of the radiation loss and the mode conversion in tapers.

Y-junctions have been investigated by subdividing them into two regions, the second of which is a taper. This last region can be designed using the results of the first section of this paper. The first region consists of the input guides which approach each other and start coupling. By using curved input guides the area taken by this coupling region can be reduced without increasing the radiation loss beyond the 3 dB for symmetrical geometries. Asymmetric junctions can be used to avoid the 3-dB loss for one input arm. However, the average of the losses for both input arms still exceeds 3 dB, unless the asymmetry is frequency or polarization dependent. Again the BPM proved suitable for computing the radiation loss in Y-junctions.

R. Baets wishes to thank the Belgian Nationaal Fonds voor Wetenschappelijk Onderzoek for a grant that enabled him to do this work.

References

1. J. A. Fleck, J. R. Morris, and M. D. Feit, Appl. Phys. **10**, 129 (1976).
2. M. D. Feit and J. A. Fleck, Jr., Appl. Opt. **18**, 2843 (1979).
3. J. Van Roey, J. van der Donk, and P. E. Lagasse, J. Opt. Soc. Am. **71**, 803 (1981).
4. G. B. Hocker and W. K. Burns, Appl. Opt. **16**, 113 (1977).
5. H. Kogelnik, *Topics in Applied Physics*, *Vol. 7* (Springer, Berlin, 1979), Chap. 2.
6. W. Streifer and E. Kapon, Appl. Opt. **18**, 3724 (1979).
7. D. Marcuse, Bell Syst. Tech. J. **49**, 273, 919 (1970).
8. N. Tzoar and R. Pascone, J. Opt. Soc. Am. **71**, 1107 (1981).
9. R. K. Winn and J. H. Harris, IEEE Trans. Microwave Theory Tech. **MTT-23**, 92 (1975).
10. A. F. Milton and W. K. Burns, IEEE J. Quantum Electron. **QE-13**, 828 (1977).
11. F. Sporleder and H. G. Unger, *Waveguide Tapers, Transitions and Couplers* (Peregrinus, Stevenage, 1979), Chap. 9.
12. J. van der Donk, Ph.D. Thesis, U. Gent, Belgium (1981).